Journal of Manufacturing Processes 141 (2025) 403–415

Contents lists available at ScienceDirect

Journal of Manufacturing Processes

journal homepage: www.elsevier.com/locate/manpro

Model based adaptive process control along intercompany process chain for sheet metal forming of steel

Nilesh Thakare [a,*], Jannik Gerlach [a], Nikita Fjodorovs [b], David Bailly [a], Emad Scharifi [a]

[a] Institute of Metal Forming, RWTH Aachen University, Intzestrasse 10, 52072 Aachen, Germany
[b] FIR e.V. at RWTH Aachen University, Campus-Boulevard 55, 52074 Aachen, Germany

ARTICLE INFO

Keywords:
Industry 4.0
Digitalization
Metal forming
Process modelling and simulation
Process optimization
Data-based manufacturing

ABSTRACT

A typical metallic product manufacturing process chain involving several companies faces challenges in promptly responding to the deviations in material properties, thereby impacting its economic efficiency. This can be attributed to the lack of knowledge about the exact condition of each product in a batch, as suppliers can only perform quality inspections randomly. This study introduces a novel approach utilizing simulation models to calculate the mechanical properties of products and design of experiments based process design using the calculated product properties shared by suppliers with their customers over a secure and reliable intercompany data management platform. The proposed approach is implemented in a laboratory scale process chain consisting of cold rolling and deep drawing using DC04 steel to demonstrate adaptive process control via intercompany exchange of yield and tensile strength of the cold strip. The benefits of adaptive process control are demonstrated by 50 % reduction in deviations in the minimum sheet thickness in cross die, thus showcasing the reproducibility of the end product with improved quality and by avoiding scrap generation, thereby allowing a sustainable manufacturing.

1. Introduction

Metallic products typically pass through process chains involving several companies such as casting, forging, hot and cold rolling, heat treatment, surface treatment, etc. These metallic products experience different conditions from the ore through intermediate states (semi-finished products) to the final states during their processing in a process chain where each company processes the semi-finished products to meet its customer requirements defined in the form of specifications. In order to stay sustainable in a competitive market, companies are required to deliver their products of higher/improved quality and productivity by efficient use of resources without violating machine and process limits [1–3]. For that purpose each company in a process chain optimizes its own process to achieve customer specifications with the help of process experts [4]. Additionally before delivering the semi-finished products, suppliers conduct quality inspections by randomly selecting a few products from a batch to ensure their compliance with specifications. Thus the properties of few randomly inspected products are representative of the entire batch [5].

However, such typical process chain has its limitations. The metal forming processes that are suitable for mass production, lack flexibility and customization [2]. Furthermore despite optimizing each individual process in a process chain, defects are generated in the form of deviations in the mechanical properties of the product [3]. Since the quality inspection for the mechanical properties of each product is not feasible, there is absence of knowledge about the exact properties of each individual product in a batch. Therefore, customers cannot rapidly adjust their own process in response to these undetected and unknown deviations in the incoming material properties [6]. These deviations, if not controlled, can propagate along the process chain, leading to scrap generation and reducing the overall economic efficiency of entire process chain [7,8]. Furthermore, today significant amount of data is generated in a process chain at different processing steps due to the advancements in digitalization and Industry 4.0 [3,9]. However, most of this data is either lost or cannot be used due to the absence of a reliable means to transfer data between the companies. Consequently, a lot of optimization potential is untapped [9,10]. Given the error-prone nature of current manual methods of data transfer via email, typically in Excel format, a shift towards reliable and secure digital solutions is necessary. This transition is crucial given the sensitivity of the exchanged information, which includes proprietary details on material specifications and process parameters critical to maintaining competitive advantage

* Corresponding author.
E-mail address: nilesh.thakare@ibf.rwth-aachen.de (N. Thakare).

https://doi.org/10.1016/j.jmapro.2025.02.082
Received 5 August 2024; Received in revised form 3 December 2024; Accepted 28 February 2025
Available online 6 March 2025

and safeguarding internal know-how. Therefore, embracing a robust data exchange mechanism is imperative for streamlining operations and enhancing collaboration within the steel supply chain [11].

To overcome above limitations, a novel approach of model based adaptive process control is investigated in the present study where firstly simulation models are used to calculate the mechanical properties of the product thereby providing information about every individual product in a batch. Secondly, in order to react to the deviations in the incoming material properties, a design of experiments based process optimization approach is implemented. Finally, for the reliable and secure sharing of mechanical properties of products between companies in the process chain, a conceptual intercompany data management platform is used. The proposed approach is implemented in a laboratory-scale demonstrator process chain, incorporating two industry-relevant metal forming steps - cold rolling and deep drawing - representing two distinct companies. The cold rolling company functions as a supplier and produces cold strip having yield and tensile strength as its properties. Whereas, the deep drawing company functions as a customer and produces cross die having minimum sheet thickness as its property. In the selected demonstrator process chain, it is successfully demonstrated that the proposed approach can help improve the quality of the deep drawn product (cross die) by reducing deviations in its minimum sheet thickness by 50 % and avoid scrap generation during deep drawing step thereby paving a way for sustainable manufacturing.

2. Approach for the investigation of adaptive process control

In order to demonstrate model based adaptive process control, four required aspects, namely an environment to conduct experiments along with a data management platform for the exchange of the mechanical properties of the products in the process chain, pseudo product specifications of the selected end product i.e. cross die, simulation models to predict cold strip and cross die properties, a method to identify process parameters using the simulation model are prepared. The benefits of model based adaptive process control is demonstrated with the help of two use cases by improving the cross die property through minimization of the deviations in its minimum sheet thickness and by avoiding the scrap generation during deep drawing. Nevertheless following assumptions and considerations are made in the presented work:

a. Process chain is selected simple enough to realize at the laboratory scale.
b. For modelling of the deep drawing process, von Mises isotropic yield criteria is used for the plastic material behaviour. However, it must be considered that the cold rolled steel sheets tend to show orthotropic behaviour. Therefore, using the isotropic yield criteria can lead to an overestimation of thinning in the cross die as against to using an orthotropic yield criteria like Hill48 as shown in Appendix A.
c. The deep drawing press used in this work has its control system that uses the set blank holder provided by the operator to accordingly control the pressure in the hydraulic cylinders. However, the force sensors that are retrofitted in the press show deviations from the set blank holder force. Therefore, for conducting the DoE and deep drawing experiments, the set blank holder force is used, while for FE deep drawing simulations, the corresponding actual force applied by the blank holder is employed (see Appendix B).

2.1. Setup of a test environment to conduct experiments

A demonstrator process chain involving of two representative companies performing cold rolling (company A) and deep drawing (company B) is selected with cross die [12] as the final product. All the necessary hardware, software infrastructure together with the information and material flow within the selected demonstrator process chain is depicted in Fig. 1.

For conducting cold rolling and deep drawing experiments, Bühler VRW-400 universal rolling mill (max. Rolling force 4000 kN, max. Rolling torque 130 kNm, max. Rolling speed 30 m/min) and Lauffer RA-250 deep drawing press (max. Press force upper piston 2500 kN, max. Press force lower piston 1250 kN, max. Press velocity 35 mm/s) are used. To determine the mechanical properties of the cold strip, tensile tests are carried out at room temperature using tensile test specimens of form H according to DIN 50125-E on the Zwick Z100 tensile testing machine (max. Tensile force 100 kN, Traverse speed 0.0005–200 mm/min) which is equipped with an optical video extensometer and GOM ARAMIS-4 M-system with a frame rate of max. 50 Hz for recording the displacement behaviour during elastic-plastic deformation. For intentionally producing a cold strip outside specifications in use-case 2 discussed in Section 2.5 to demonstrate adaptive process control, annealing of cold strips is conducted using the Nabertherm N761 furnace (max. Temperature 1200 °C, max. Volume 800 mm * 1900 mm * 500 mm width*depth*height). Minimum thickness in the cross die is identified by first cutting of the cross die using a sawing machine from August Mössner GmbH followed by the thickness measurement using a digital Vernier calliper as shown in Appendix A. To simulate two collaborating companies in a supply chain, two different NoSQL databases (mongoDB and ArangoDB) are set up. A prototype platform is developed for this purpose based on industrial specific requirements outlined in [11]. This platform incorporates metadata to track data location and facilitates seamless data extraction from company A's database to company B's database upon request. Furthermore, the platform provides an output interface to verify the transferred data. The challenge of hosting and maintaining such a platform solely within one company is recognized due to potential high costs and concerns about possible data misuse. Therefore, the platform was hosted on the external server of the IT service provider, imitating a neutral third party such as a local or global association, offering data exchange services for a proportional fee to its members while representing the collective interests of the entire process chain.

2.2. Determination of the deviations in cold strip and cross die properties

Since the selected end product i.e. cross die is not a standard industry product, pseudo specification for cross die is required to be defined. In the deep drawing of sheet metal, normal anisotropy which is also referred as Lankford coefficient or r value is considered while selecting the material. Materials having higher normal anisotropy (r-value >1) are optimum for deep drawing process because more material flows from width direction into the length direction of the sheet than from the thickness direction due to the large resistance of the sheet against reduction in its thickness. Hence DC04 steel is selected that typically has r-value ≥ 1.6. For this work, DC04 cold strip of 1.0 mm thickness are procured from three different steel suppliers to later use them for all experiments and are characterized for their yield and tensile strength using uniaxial tensile tests as shown in Appendix D. First, trial deep drawing experiments are conducted for each of the three procured cold strips where the set blank holder force is varied between 0 kN to 600 kN and square blank edge length is varied between 240 mm to 270 mm to produce crack free and wrinkle free cross dies having a depth of 50 mm. On the basis of these trial experiments, default deep drawing process consisting of two parameters i.e. square blank with edge length of 270 mm and set blank holder force of 200 kN is selected. Finally, out of all the previously produced cross dies for each of the three cold strips, the cross die sample produced using above selected standard deep drawing process are characterized to determine the minimum sheet thickness by cutting each cross die along the three symmetry lines [12] shown in Fig. 2 using the sawing machine and measuring the thickness using Vernier calliper shown in Appendix A. Thus minimum sheet thickness in cross die represents the thickness of the thinnest region in the cross die. In other words it represents the location in cross die where maximum

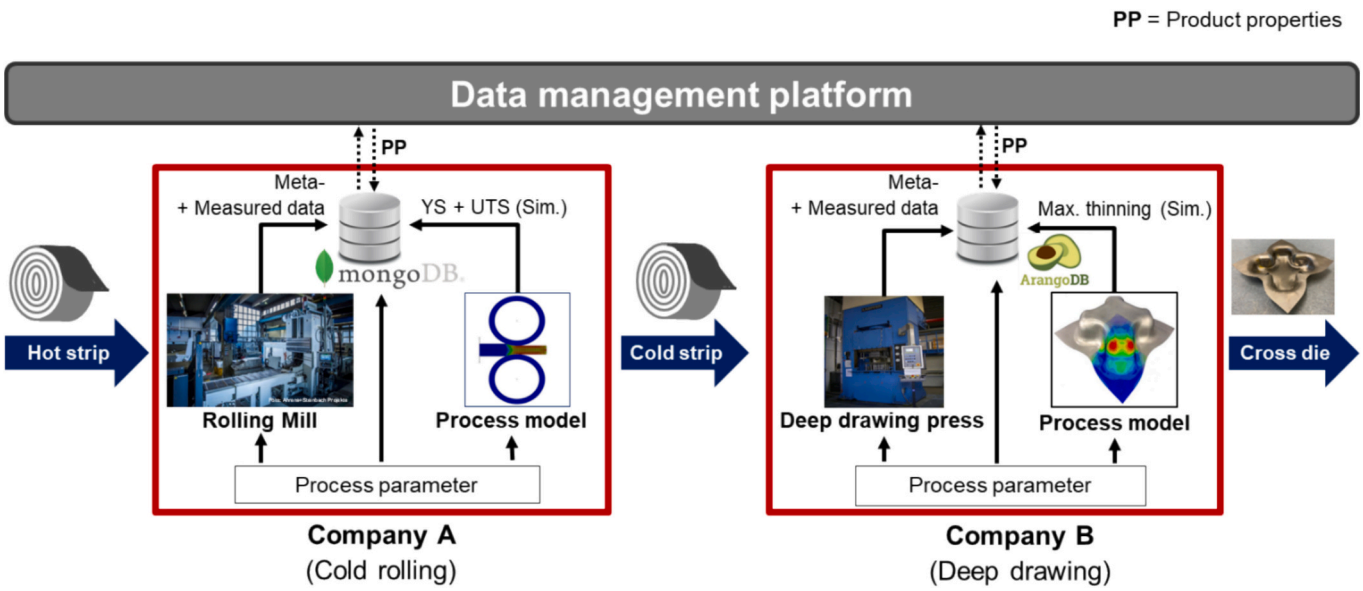

Fig. 1. An industry relevant demonstrator process chain consisting of cold rolling and deep drawing steps along with all the necessary hardware-, software components and an inter-company data platform.

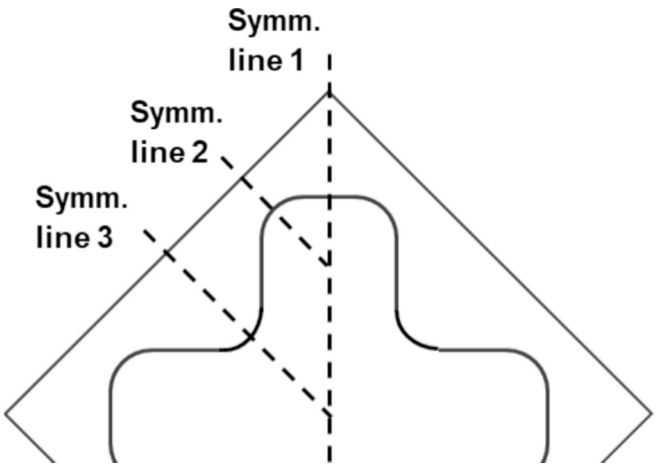

Fig. 2. Symmetry lines for measuring the thickness distribution in a cross die.

thinning is occurring. Finally the results of the characterization of each procured cold strip and respective cross die are analysed.

2.3. Modelling of cold rolling and deep drawing process

For the determination of cold strip and cross die properties, simulation models are required. The cold rolling process is modelled using the elementary strip theory based fast analytical hot rolling model (FRM) developed at the Institute of Metal Forming (IBF) that is further adapted and extended for cold rolling application. The FRM is developed in a modular fashion which consists of a process module that predicts material deformation in terms of strain and strain rate as well as force and torque during rolling, a temperature module that accounts for the thermal effects in hot rolling, and a material module that describes the material behaviour cast into equations for strain hardening, softening and microstructure evolution. The rolling force is calculated using the formula according to SIEBEL [13,14].

$$F = l_d \cdot b \cdot k_{fm} \cdot Q_p$$
$$Q_p = f\left(\mu, \frac{l_d}{h_m}\right) \tag{2-1}$$

where l_d is contact length, b is strip width, k_{fm} is mean flow stress, h_m is the mean strip thickness, μ is the coefficient of friction and Q_p is a geometry factor that is a function of $\frac{l_d}{h_m}$ and μ, which is determined using the FE simulation study whose results are shown in Appendix C. The rolling moment (M) is calculated with the help of SIMS formula where rolling force (F), contact length (l_d) and lever arm (m) are used [13].

$$M = F \cdot l_d \cdot m$$
$$m = C_1 + \frac{C_2}{C_3 + C_4 \cdot {h_0}^3} \tag{2-2}$$

Modelling of the material behaviour is done using strain, strain rate and temperature dependent flow curve according to Hensel and Spittel [13].

$$k_f = A \cdot \dot{\varphi}^{A_1 + A_2 \cdot \vartheta} \cdot e^{A_3 \cdot \vartheta} \cdot \varphi_{acc}^{A_4} \cdot e^{A_5 + \varphi_{acc}} \tag{2-3}$$

where $\dot{\varphi}$ is the strain rate, ϑ is the workpiece temperature, φ_{acc} is the accumulated equivalent strain after the previous rolling passes and A_{1-5} are the fitting parameters that are determined using the flow curves obtained with the help of the compression tests that are conducted at different strain rates and temperatures. The thermal behaviour of the workpiece is modelled using Fourier's law that is solved using finite difference methods [13].

$$\rho \cdot c_p \cdot \frac{\partial \vartheta}{\partial t} = \lambda \cdot \left(\frac{\partial^2 \vartheta}{\partial y^2}\right) + \dot{Q} \tag{2-4}$$

where ρ is density, c_p is specific heat capacity, λ is the thermal conductivity, $\dot{Q}$ is the internal heat generation. During the rolling process, the equivalent strain (φ_{eq}) and strain rate ($\dot{\varphi}$) is calculated using the below equations [13].

$$\varphi_{eq} = \frac{2}{\sqrt{3}} \cdot ln\frac{h_0}{h_1} \tag{2-5}$$

$$\dot{\varphi} = \frac{v_{roll}}{l_d} \cdot \varphi \tag{2-6}$$

where h_0 is the initial workpiece height, h_1 is the final workpiece height, v_{roll} is the work roll velocity. In order to consider the strain hardening and softening happening during forming, accumulated strain and rest

strain are used [13].

$$\varphi_{acc,i} = \varphi_{eq,i} + \varphi_{rest,i-1} \tag{2-7}$$

$$\varphi_{rest,i} = \varphi_{acc,i} \cdot (1 - X_i) \tag{2-8}$$

where $\varphi_{acc,i}$ is the accumulated equivalent strain, $\varphi_{rest,i-1}$ is rest equivalent strain and X_i is fraction recrystallized after time t seconds. Static recrystallization is considered with the help of JMAK equations to calculate grain size and recrystallized fraction [13].

$$X = 1 - exp\left(ln(0.5) \cdot \left(\frac{t}{t_{50}} \right)^k \right) \tag{2-9}$$

$$t_{50} = B \cdot d_0^{B_1} \cdot \varphi_{acc}^{B_2} \cdot exp\left(\frac{Q_{RX}}{R \cdot T} \right) \tag{2-10}$$

$$d_{RX} = C \cdot d_0^{C_1} \cdot \varphi_{acc}^{C_2} \tag{2-11}$$

$$d = X^{4/3} \cdot d_{RX} + (1 - X)^2 \cdot d_0 \tag{2-12}$$

$$d_{KW}^{D_1} = d_{RX}^{D_1} + D \cdot t \cdot exp\left(-\frac{Q_{KW}}{R \cdot T} \right) \tag{2-13}$$

where X is the recrystallized fraction after time t, k is the Avrami exponent that describes the rate of recrystallization, t_{50} is the half-life of recrystallization, Q_{RX} is the activation energy for recrystallization, T is absolute workpiece temperature, d_0 is initial austenite grain size in micrometer, d_{RX} is recrystallized grain size, d is average grain size, d_{KW} is grain size during grain growth after the complete recrystallization [13]. $B, C, Q_{KW}, D, (B_{1-2}, C_{1-2})$ are the material dependent parameters that are taken from the study conducted by Sellars & Whiteman [15]. Since cold rolling is conducted below recrystallization temperature where microstructure evolution does not takes places, the recrystallization and microstructure evolution modules are not used for the modelling the cold rolling process.

The fast cold rolling model is further extended to also calculate cold strip yield and tensile strength, using Vickers hardness based analytical models [16,17] as shown in equation from 2–14 to 2–16.

$$H_v = k \cdot c \cdot (\varphi_{eq})^n \tag{2-14}$$

$$YS = a_0 + a_1 \cdot H_v \tag{2-15}$$

$$UTS = b_0 + b_1 \cdot H_v \tag{2-16}$$

where H_v is Vickers hardness [HV], YS is yield strength [MPa], UTS is tensile strength [MPa], φ_{eq} is equivalent plastic strain, and (a_0,a_1,b_0,b_1,c, k) are the fitting parameters. After finishing the implementation and calibration of the fast rolling model, it is validated for its accuracy by comparing the simulation results with experimental results for rolling force as well as cold strip hardness, yield, and tensile strength. For this purpose, a test cold rolling experiment is conducted at room temperature using a hot strip with dimensions of 400 mm * 300 mm * 3.8 mm (L*W*H) and a pass schedule shown in Table 1.

The deep drawing process is modelled using an FE model, where only one fourth of the actual geometry is modelled as shown in Fig. 3. For this Abaqus/Standard (implicit solver) is used that is available in Abaqus 2019. The model consists of a die, blank holder and punch that are modelled as rigid parts whereas the steel blank is modelled as a deformable part using S4R shell elements with the element size of 2 mm determined using the results of a convergence analysis shown in Appendix E.

Table 1
Pass schedule used for conducting the cold rolling experiment at the Institute of Metal Forming to produce cold strip of thickness 1.0 mm.

Pass	0	1	2	3	4	5
Thickness [mm]	3.80	2.75	2.05	1.55	1.15	1.00
Roll speed [m/min]	7.2					
Work roll radius [mm]	80					

The cold strip plastic behaviour is extrapolated for higher strains using McConnell-Lenard flow curve shown in Eq. (2-17) while the Young's modulus of 210 MPa and Poisson's ratio of 0.3 is defined.

$$\sigma = A \cdot (1 + B \cdot \varphi)^C \tag{2-17}$$

The die is held fixed in its position using the ENCASTRE boundary condition. A constant blank holder force which equals the applied blank holder force in the corresponding experiment is applied in negative Z direction on the blank holder while the punch velocity of 5 mm/s is defined in negative Z direction for its downward movement. XSYMM symmetry boundary condition is applied on the square blank edge along the y axis and YSYMM symmetry boundary condition is applied on the square blank edge along the x axis as shown in Fig. 3 b). For modelling the contact between sheet and rest of the parts, general contact interaction (surface-to-surface contact in Abaqus) is used where all the master surfaces are defined on rigid parts while slave surfaces on the deformable sheet part. Additionally, a tangential behaviour using penalty friction formulation with coefficient of friction of 0.05 and a normal behaviour with exponential pressure-overclosure is defined. Next the deep drawing model is validated for its accuracy by comparing the simulation results with experiments conducted in Section 2.2. Finally, a sensitivity analysis is conducted where the influence of variations in set blank holder force, square blank edge length and friction coefficient on the max. deep drawing force and min. sheet thickness are analysed as shown in Appendix E.

2.4. Deep drawing process design and optimization using design of experiments

With the availability of knowledge about the deviations in the cold strip yield and tensile strength, Design of Experiment (DoE) is used to determine the deep drawing process parameters to help representative company B in the design of its process configuration to produce cross die that meet the specification. The DoE workflow is shown in Fig. 4.

Starting with the cold strip properties shared by representative company A over data management platform together with upper and lower limits of deep drawing process parameters, namely square blank edge length and set blank holder force, number of simulations to be conducted and target cross die property, are used as the input for the DoE. The Full Factorial Design (FFD) method [18–21] generates samples equal to the number of simulations within the user defined design space. Subsequently, a FE deep drawing model is created for each of the DoE samples, simulation is started and results are extracted upon its completion. Finally using the provided target value, each sample is categorized as ok (green sample) and nok (red sample).

2.5. Benefits of model based adaptive process control

After setting up the test environment with all its hardware and software components described above, the benefits of model based adaptive process control are demonstrated with the help of the following two use cases.

Use case 1: Minimization of deviations in the minimum sheet thickness in cross die.

The aim of the first use case is to improve cross die quality by reducing the variation in minimum sheet thickness in the cross die. For this purpose, first DoE is conducted for each of the previously procured cold strips from the three steel suppliers by using their material properties to determine the deep drawing process

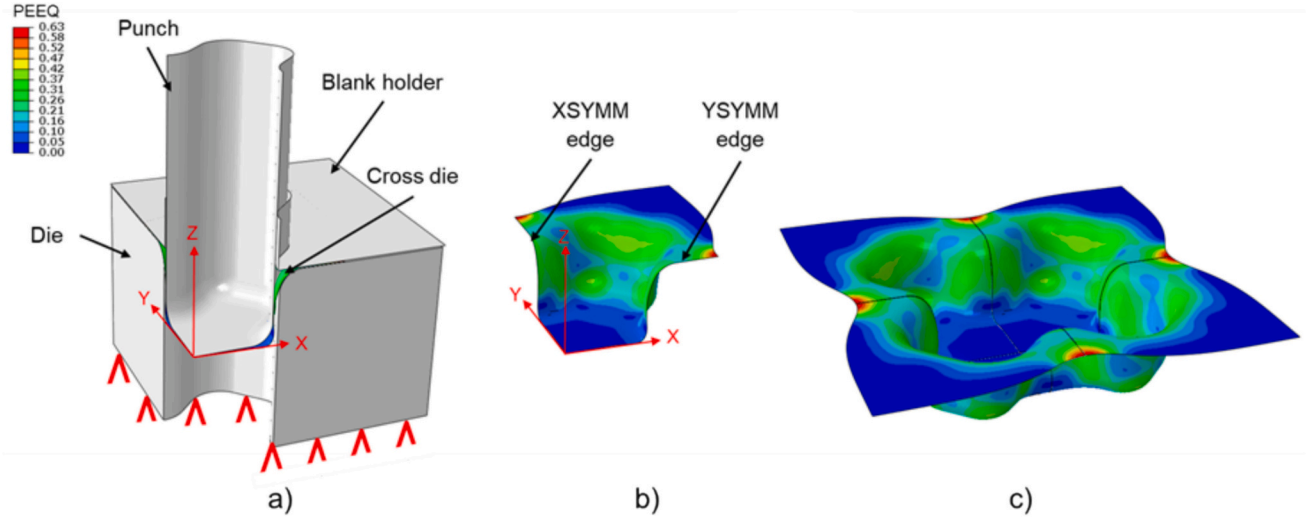

Fig. 3. FE deep drawing model showing the distribution of equivalent plastic strain (PEEQ) in cross die a) one fourth deep drawing model including punch, die, blank holder and cross die b) one fourth cross die at the end of deep drawing c) complete cross die mirrored around z axis.

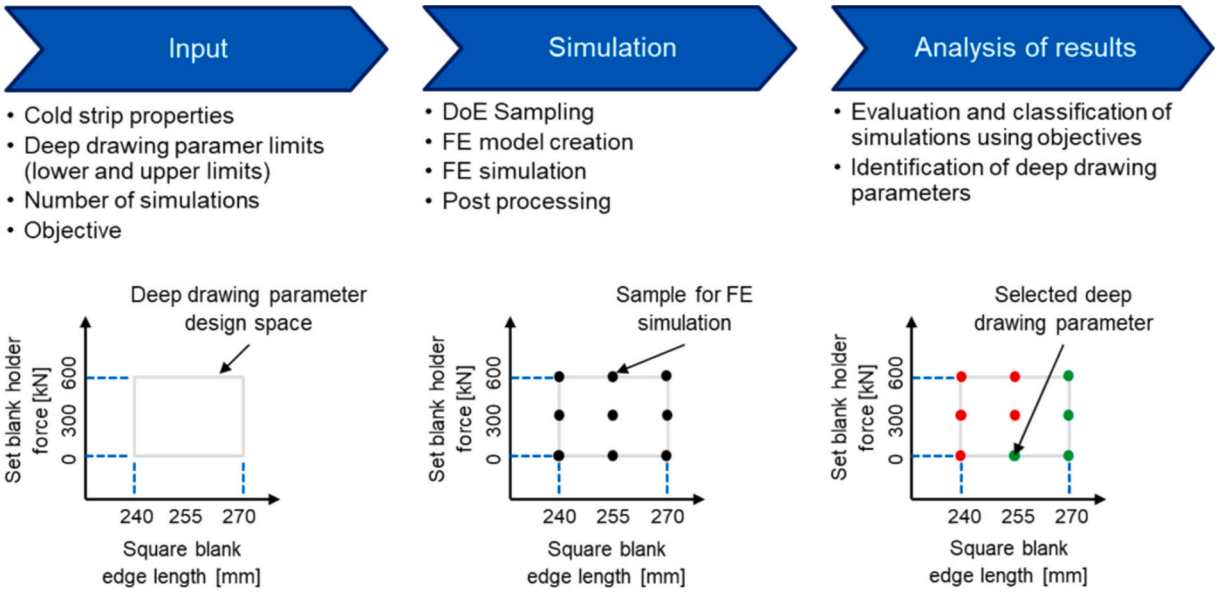

Fig. 4. The workflow for determination of deep drawing parameters using user defined inputs, DoE method and the validated deep drawing FE model.

parameters. For that, set blank holder force is varied in 4 levels i.e. 0 kN, 200 kN, 400 kN and 600 kN while the square blank edge length is varied in 3 levels i.e. 240 mm, 255 mm and 270 mm. Finally using the selected deep drawing process, cross dies are produced and characterized to determine their minimum thickness.

Use case 2: Reduction of scrap generation during deep drawing.

The goal of the second use case is to avoid scrap generation during deep drawing. To achieve this, a 3.8 mm thick hot strip is cold rolled to 1.0 mm thickness using the pass schedule presented in Section 2.3 and annealed for 8 Hrs at 700 °C to produce a cold strip with the yield and tensile strength outside its specifications. The aim lies in producing material with increased yield strength while leaving the ultimate tensile strength untouched. As a result, the material shows reduced work hardening leading to larger thinning levels in cross die after the deep drawing step. This is due to lower hardening capacity in already thinned areas and therefore less resistance against further thinning as the consequence of plastic deformation compared to the material within specification. Finally, the DoE is conducted using the annealed cold strip material properties to determine the new deep drawing process parameters. Using the new deep drawing process, it is shown that even cold strip outside specifications can be processed to produce good cross die.

3. Results and discussion

3.1. Determination of the deviations in cold strip and cross die properties

The results of all the material characterizations and deep drawing experiments using three different DC04 cold strips with 1.0 mm thickness are summarized in Table 2. DC04 cold strips procured from three different suppliers show significant difference in the yield strength from 169 MPa to 193 MPa (a difference of 12.4 %), where the tensile strength values are approximately at the same level ranging from 284 MPa to 294 MPa (a difference of 3.4 %). However, despite using same default deep drawing process, the differences in cold strip properties (difference in the work hardening) cause difference in minimum thickness in cross die

Table 2
Summary of characterized cold strips properties using uniaxial tensile tests and respective cross die properties using thickness distribution along with the used default deep drawing process parameters.

Steel supplier		A	B	C
DC04 cold strip specifications	Yield strength [MPa]	140–210		
	Tensile strength [MPa]	270–350		
Procured cold strip properties	Yield strength [MPa]	178	193	169
	Tensile strength [MPa]	294	286	284
Default deep drawing process parameters	Square blank edge length [mm]	270		
	Set blank holder force [kN]	200		
Cross die property	Min. sheet thickness [mm]	0.74	0.70	0.72

ranging from 0.70 mm to 0.74 mm (difference of 13.4 % in thinning), as shown in Table 2. For each cold strip the difference between yield and tensile strength represents the amount of work hardening. Cold strip B, which demonstrates lower work hardening, leads to the highest thinning in cross die resulting in min. Sheet thickness of 0.7 mm. Cold strip A, which shows higher work hardening, leads to the lowest thinning in cross die resulting in min. Sheet thickness of 0.74 mm.

The results of the material characterization confirm the hypothesis that, despite procuring cold strips with identical specifications, there are deviations in the cold strip properties. These deviations propagate along the process chain to cause significant deviations in the cross die property when processed with the same default deep drawing process parameters. Thus showing the need of model based adaptive process control to make it possible to react to the deviations in cold strip properties. The results from above experiments provide a foundation for the demonstration of adaptive process control in Section 3.3. Observing the values for minimum sheet thickness in cross dies from Table 2, pseudo specification for cross die is defined such that its lower limit is equal to smallest value for minimum sheet thickness among all three cross dies i.e. 0.7 mm whereas upper limit is defined as 1.0 mm representing cross die without any thinning present in it. For better understanding and visualisation of the results obtained, Fig. 5 shows the upper and lower limits of DC04 specifications (black line) and of deviations in procured DC04 cold strip mechanical properties (red line). Similarly Fig. 5 shows lower and upper limits of cross die pseudo specifications (black line) and of deviations in minimum sheet thickness in cross die (red line) as a result of deviations in cold strip mechanical properties.

3.2. Modelling of the cold rolling and deep drawing process

The Vickers hardness based analytical model for cold strip properties is calibrated using Matlab curve fitting toolbox as shown in the Eqs. (3-1) to (3-3).

$$H_v = 1200 \cdot 0.1807 \cdot (\varphi_{eq})^{0.218} \tag{3-1}$$

$$YS = -282.2 + 4.435 \cdot H_v \tag{3-2}$$

$$UTS = -203.6 + 4.157 \cdot H_v \tag{3-3}$$

After calibrating all the model parameters, the cold rolling model is validated for rolling force, yield and tensile strength with the help of experimental results obtained from a test cold rolling experiment conducted using a pass schedule presented in Section 2.3. The simulation results, shown in Fig. 6, display a good accuracy with a relative error <10 % for rolling force and cold strip mechanical properties.

In Fig. 7, the results of the deep drawing model i.e. maximum deep drawing force and minimum sheet thickness in the cross die, are compared with deep drawing experiments conducted in Section 2.2. The comparison demonstrates that model accurately simulates the deep drawing process for all three cold strips while using the default process parameters. The relative error for predicted and experimental maximum deep drawing force and minimum sheet thickness in cross die is less than 5 %.

The validation results for both the cold rolling and deep drawing models demonstrate good agreement with the experiments. Hence these models can be used for simulating cold rolling and deep drawing process to determine cold strip yield and tensile strength as well as minimum sheet thickness in cross die. Thus allowing the simulation of different processes parameter combinations to identify best process even before conducting experiments. Both the validated model are integrated in the complete test environment as described in Section 2.1.

3.3. Demonstration of the model based adaptive process control

The implementation of the proposed approach together with the validated simulation models and DoE method is finally used in the realization of model based adaptive control where the representative company B is able to react to the deviations in mechanical properties of incoming cold strip shared by representative company A using inter-company data exchange platform. The benefits of adaptive process control are demonstrated with the help of selected use cases.

Use case 1: Minimization of deviations in the minimum sheet thickness in the cross die.

In order to determine the new deep drawing process fulfilling the specifications, a DoE is conducted using the material properties of each of the three cold strips having different hardening behaviour. The results

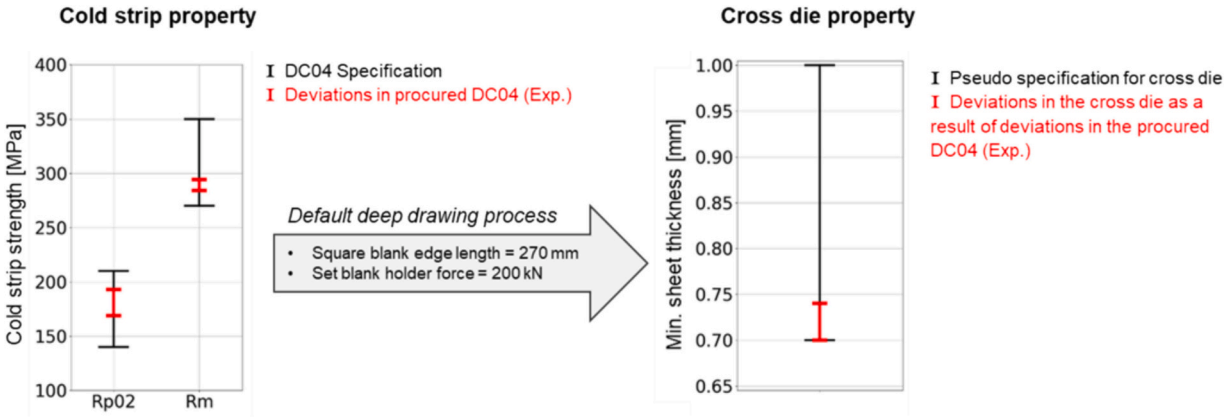

Fig. 5. Deviation in the cold strip and cross die properties and the pseudo specifications of the cross die determined using DC04 steel procured from three different suppliers.

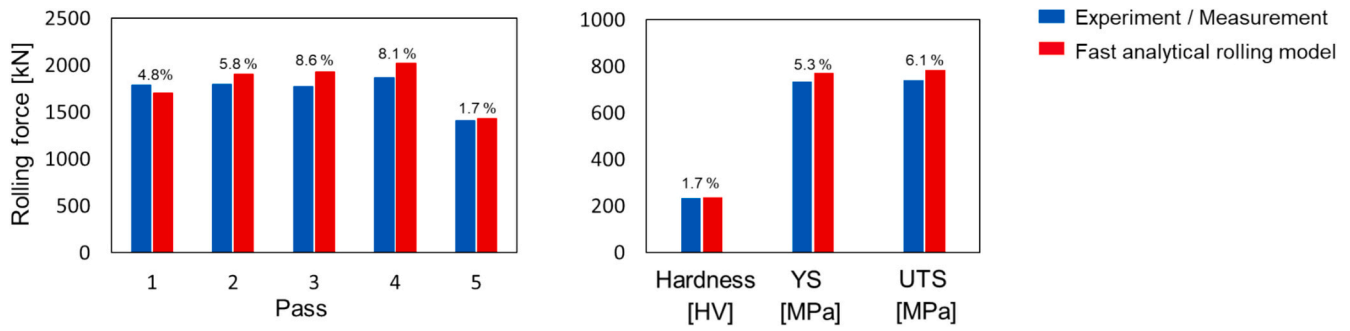

Fig. 6. Validation of cold rolling model using rolling force, cold strip hardness, yield- and tensile strength obtained experimentally.

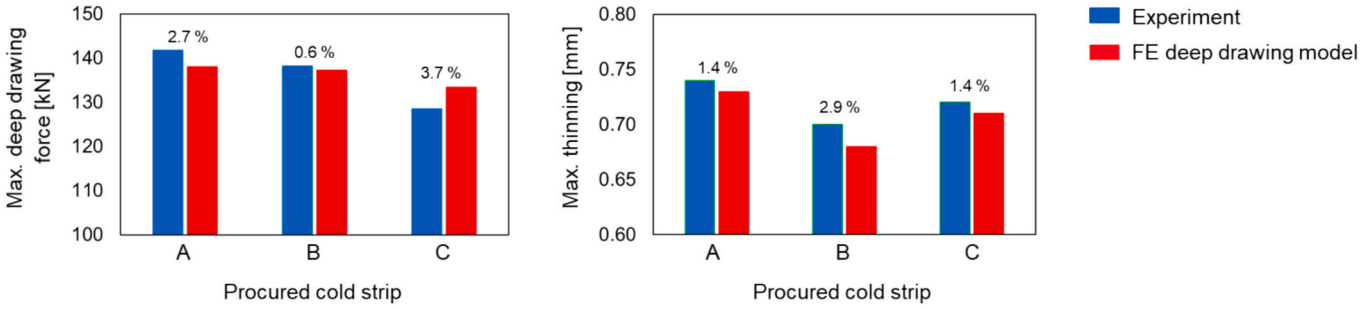

Fig. 7. Validation of deep drawing FE model using max deep drawing force and max. Thinning obtained experimentally.

of DoE are shown in Fig. 8. Red samples indicate cross die that do not fulfil specifications, while green samples represent cross die that meet specifications.

Based on the DoE results, the deep drawing process parameters are aimfully selected with the goal of minimizing the deviations in minimum sheet thickness in cross die. The selected process parameters are then used to conduct deep drawing experiment for each cold strip. The produced cross dies are shown in Fig. 9.

Finally the produced cross dies are characterized for their minimum sheet thickness. The experimental results demonstrate that the proposed approach managed to minimize the original cross die deviations presented in Section 3.1 by 50 % from 0.70 mm to 0.74 mm to 0.73 mm to 0.75 mm. The used deep drawing parameters and corresponding minimum sheet thickness in cross die are summarized in Table 3.

The results of this use case successfully show how the availability of knowledge about exact properties of incoming cold strip helps representative company B modify its deep drawing process with the help of DoE suggested deep drawing parameters such that the cross dies with desired properties can be produced. Additionally, the results indicate that the representative company B can produce cross dies with smaller deviations in their properties compared to when using the default deep drawing process. Thus enabling improved product quality and improved economic efficiency, as any deviations in the cold strip caused by upstream processing steps will not propagate downstream in the process chain.

Use case 2: Reduction of scrap generation during deep drawing

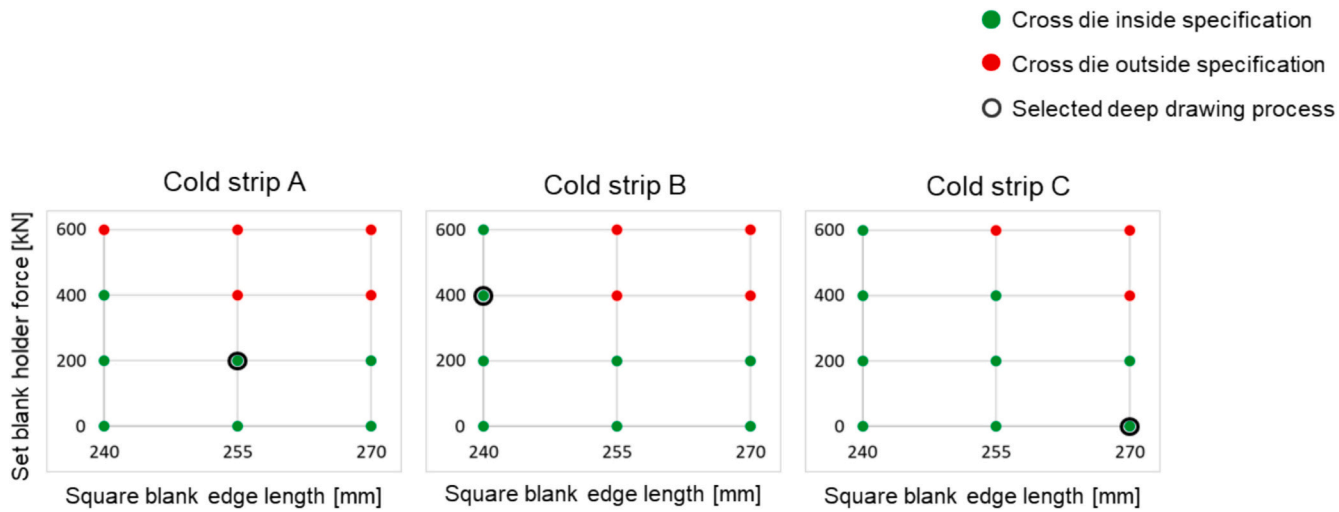

Fig. 8. Results of the DoE conducted for each cold strip where square blank edge length is varied between 240, 255 and 270 mm and set blank holder force is varied between 0, 200, 400 and 600 kN; red samples indicate cross die not fulfilling the specifications whereas green samples indicate cross die fulfilling the specifications. (For interpretation of the references to colour in this figure legend, the reader is referred to the web version of this article.)

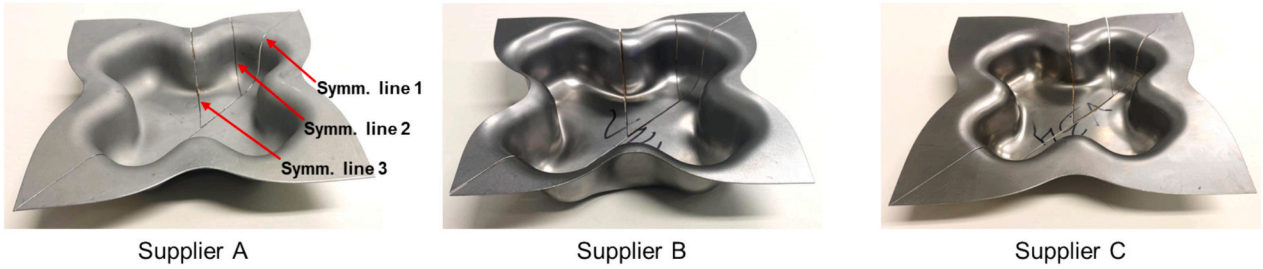

Fig. 9. Cross dies produced from three procure cold strips using the deep drawing process selected from the DoE results shown in Fig. 8.

Table 3
DoE based determination of the deep drawing parameters for reducing deviations in cross die property.

Steel supplier			A	B	C
Deep drawing parameter	Square blank edge length [mm]		255	240	270
	Set blank holder force [kN]		200	400	0
Cross die property	Min. sheet thickness [mm]	Sim.	0.74	0.72	0.74
		Exp.	0.73	0.75	0.74

For this use-case, a cold strip outside its specification is produced at the Institute of Metal Forming as per Section 2.5 and characterized using uniaxial tensile tests resulting in yield strength of 240 MPa and tensile strength of 310 MPa. The difference between yield strength and ultimate tensile strength is reduced by 35 % compared to the material within specifications, indicating a lower work hardening in the new material. As shown in Fig. 10, deep drawing simulation shows that processing the above mentioned cold strip using the default deep drawing process (square blank edge length = 270 mm and set blank holder force = 200 kN) produces cross die with minimum sheet thickness of 0.66 mm.

Since 0.66 mm is below the lower limit of the pseudo cross die specification i.e. 0.70 mm, the resulting cross die would lie outside specification thereby making it a scrap. In this case, the larger thinning is directly linked to the lower work hardening in the material, since already thinned areas in the sheet harden less and therefore show less resistance against further thinning. To avoid generation of scrap, the proposed approach of adaptive process control is used to allow processing of above cold strip by suggesting the new deep drawing process parameters to produce good cross die. Accordingly, DoE suggested new deep drawing process with square blank edge length of 245 mm and set blank holder force of 0 kN are selected. Suggested parameters are then used to conduct deep drawing experiments to produce a wrinkle free cross die, which is characterized for its minimum sheet thickness by measuring sheet thickness along the three symmetry lines as shown in Fig. 11.

Results of cross die characterization indicate a minimum sheet thickness of 0.77 mm which is above the lower limit of 0.70 mm thereby making it a good part. The modified deep drawing process and cross die properties are shown in Fig. 12.

The results of this use case successfully demonstrated how the availability of knowledge about exact properties of incoming cold strip help representative company B to modify their deep drawing process such that even the cold strip outside specifications can be processed. Thus allowing companies to continue production even in the situations where different material needs to be used to meet the customer deadlines during material shortage caused by the problems in the supply chains. Thus companies can buy material with wider or different specifications thereby allowing monetary savings on the purchase of material. This can help companies stay competitive in the market.

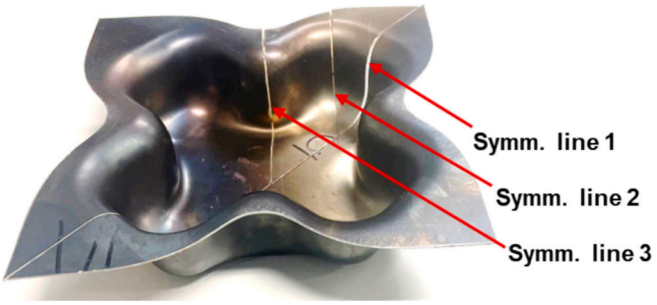

Fig. 11. Cross die produced using the DoE suggested deep drawing process for the cold strip produced at the Institute of Metal Forming characterized regarding thickness distribution along three symmetry directions.

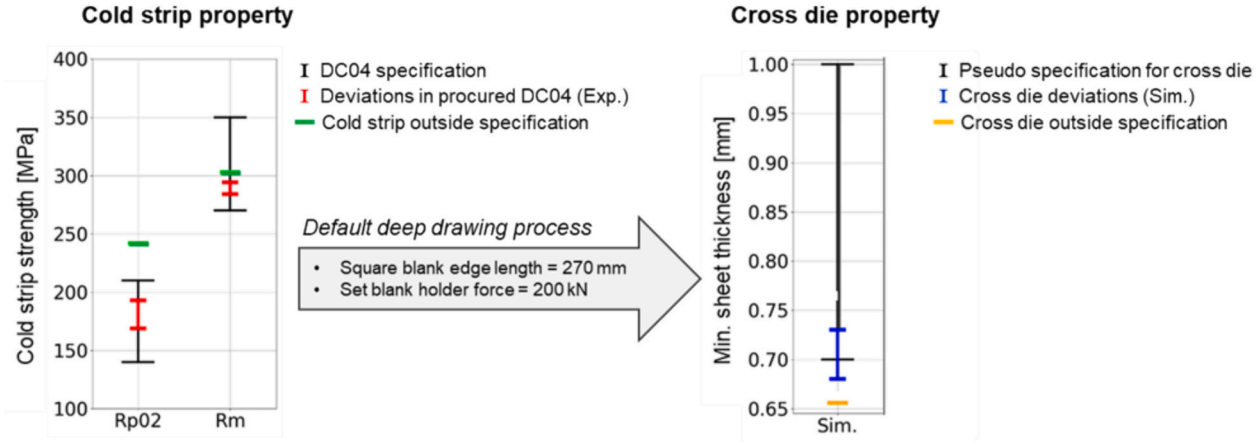

Fig. 10. Simulation of the default deep drawing process when processing a cold strip outside the specification produced at the Institute of Metal Forming. Default processing leads to producing a cross die with min. Thickness of 0.66 mm that lies below the lower limit of 0.70 mm.

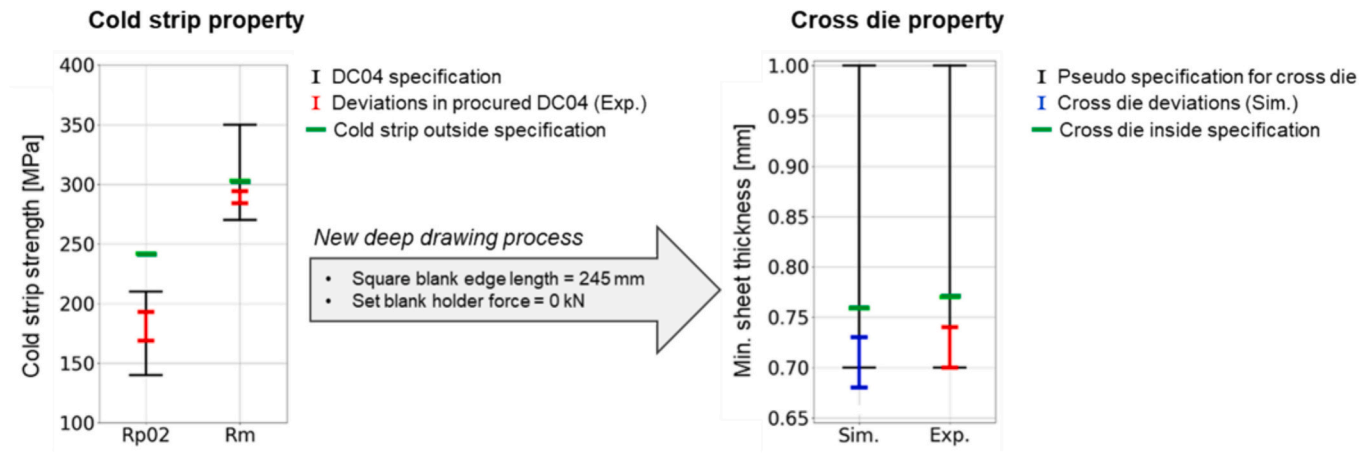

Fig. 12. Determination of a new deep drawing process using DoE to avoid scrap generation followed by conducting deep drawing experiment for validation. Adapted processing leads producing cross die with min. Thickness of 0.77 mm that lies above the lower limit of 0.70 mm.

4. Conclusion

In industrial steel process chains, only a few parts in a batch are randomly selected to determine the mechanical properties of products. The resulting uncertainty about the overall properties of the formed products lead to undetected deviations, which are carried forward through the process chain and can result in scrap generation since process configuration cannot be adapted accordingly. This work aims to demonstrate how a model based prediction of mechanical properties for each individual formed product can be used for adaptive process control downstream in the process chain. This can help avoid scrap generation and furthermore decrease deviations in product properties, thus resulting in increased product quality.

To achieve this, a model process chain containing of two companies is set up, where a cold rolling company functions as supplier while a deep drawing company functions as a customer. The cold strips of the same specification i.e. DC04 are procured from three different industrial suppliers to substantiate the underlying hypothesis of this work. In a first step, the mechanical properties, namely yield strength and ultimate tensile strength, of these cold strips are characterized using uniaxial tensile tests where deviations of up to 12.4 % in yield strength are determined despite having the same specifications. The cold strips are passed on to the deep drawing company, where cross dies are produced using same default deep drawing process parameters for each cold strip. As a result, cross dies with up to 13.4 % difference in maximum observed thinning were produced.

To overcome this, two use cases are carried out, demonstrating the potential of model based adaptive process design. Both companies are supplied with suitable simulation models to predict the mechanical properties of cold strips after cold rolling and minimum sheet thickness in cross die after deep drawing. For process adaption, the Design of Experiments (DoE) approach is implemented in the deep drawing company. The first use case successfully demonstrated how the knowledge of the exact cold strip properties can be used to increase product quality during cross die production. Using model based approach, deviations in minimum sheet thickness are reduced by 50 %. In second use case, the cold rolling company intentionally produced cold strips outside specification with increased yield strength, leading to reduced work hardening in the material and benefiting the thinning in the cross die. It was demonstrated that by not adapting deep drawing parameters, cross dies with thinning higher than allowed by the defined specification are produced, resulting in scrap generation. By using proposed model based adaptive approach, deep drawing parameters could be determined that lead to production of cross die with thinning within the specification, thus preventing generation of scrap.

To summarize, the present study illustrates how model based adaptive process design can be used to overcome the uncertainties in the incoming mechanical properties and result in production of products with higher quality, increasing competitiveness of companies. Additionally, it is demonstrated that even material outside specification can be used for producing products within the defined specifications, thus preventing scrap generation and increasing sustainability of the whole process chain.

CRediT authorship contribution statement

Nilesh Thakare: Writing – original draft, Visualization, Validation, Software, Methodology, Investigation, Formal analysis, Data curation, Conceptualization. **Jannik Gerlach:** Writing – review & editing, Methodology, Conceptualization. **Nikita Fjodorovs:** Writing – review & editing, Methodology, Conceptualization. **David Bailly:** Writing – review & editing, Supervision. **Emad Scharifi:** Writing – review & editing, Supervision.

Declaration of competing interest

The authors declare that they have no known competing financial interests or personal relationships that could have appeared to influence the work reported in this paper.

Acknowledgement

This work is part of the IGF project 21590 N of the FOSTA e. V. funded by the AiF within the framework of the programme for the promotion of joint industrial research (IGF) by the German Federal Ministry for Economic Affairs and Climate Action on the basis of a resolution of the German Parliament. The authors would like to acknowledge the contributions of Prof. Dr.-Ing. Gerhard Hirt and late Dr.-Ing. Johannes Lohmar to this work. Their expertise and feedback was instrumental in the completion of this work.

Appendix A. Measurement of the cross die thickness

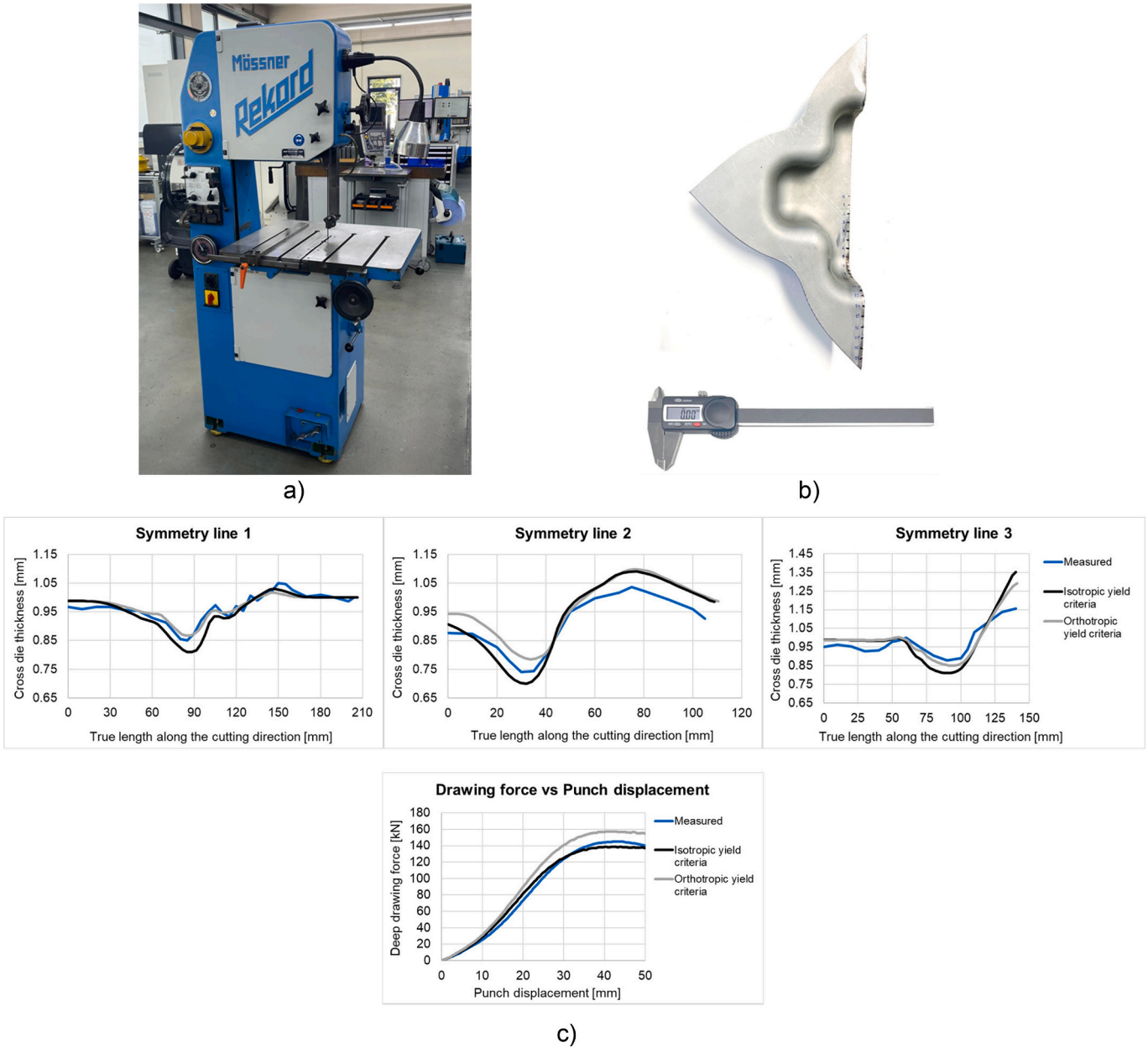

Fig. A.1. Measurement of the cross die thickness a) sawing machine from Mössner GmbH for cutting the cross die samples, b) a digital Vernier calliper for measuring the cross die thickness at the locations marked at the distance of 10 mm (in the flat regions) and 5 mm (in the curved regions) along the cut edge of the cross die, c) Comparison of the thickness distribution measured along three symmetry directions and drawing force vs punch displacement – measured, FE simulation with isotropic yield criteria and FE simulation with orthotropic yield criteria defined using the Hill anisotropic plasticity potential for planar anisotropy with stress ratios R11 = R12 = R23 = 1.0, R22 = 0.992, R33 = 1.162, R12 = 1.14.

Appendix B. Deep drawing experimental setup

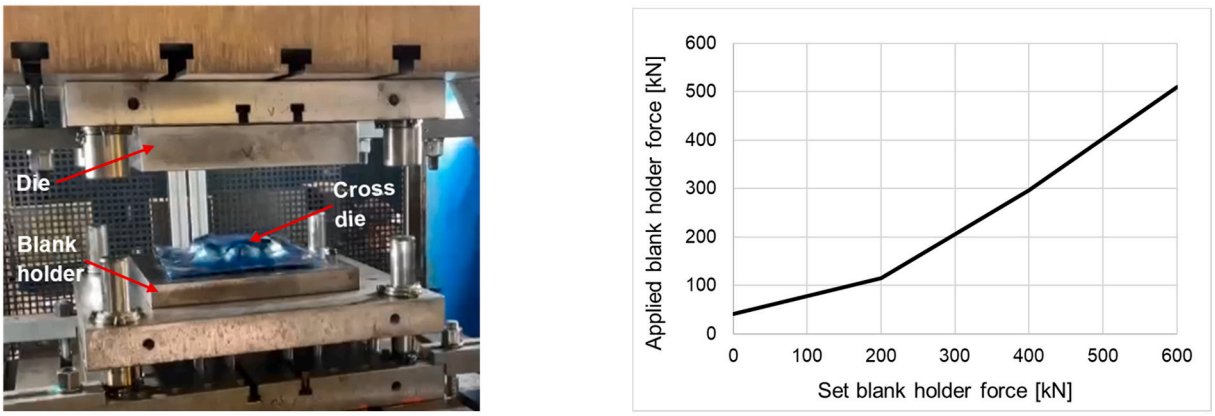

Fig. B.1. a) Deep drawing press with upper piston causing die to move in the downward direction whereas lower piston applying upward force on the blank holder. The square blank is covered with blue plastic foil (blue colour) and lubricating oil is applied to promote the deformation by reducing friction, b) Representation of the difference in the set blank holder force provided by the press operator and the applied blank holder force measured using the retrofitted force sensors. (For interpretation of the references to colour in this figure legend, the reader is referred to the web version of this article.)

Appendix C. Cold rolling model calibration

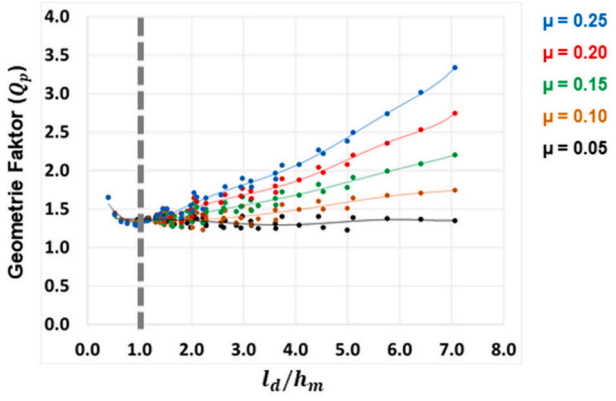

Fig. C.1. Results of FE simulation study conducted for coefficient of friction ranging from 0.05 to 0.25 and different height reductions ranging from 5 % to 40 %. The geometry factor (Q_p) is calculated inversely using the rolling force formula acc. to SIEBEL (Eq. (2-1)).

Table C.1
Model for geometry factor (Q_p) fitted using the results of FE simulation study and the curve fitting toolbox available in Matlab.

Model validity	Model for geometry factor	R^2	RMSE
$\left(\frac{l_d}{h_m}\right) < 1$	$Q_p = 0.0901 + 0.7664\cdot\left(\frac{l_d}{h_m}\right) + 0.5029\cdot\left(\frac{h_m}{l_d}\right) + 0.1482\cdot\mu + 0.0602\cdot\left(\frac{1}{\mu}\right) - 0.3816\cdot\left(\frac{l_d}{h_m}\right)\cdot\mu$	0.98	0.01
$\left(\frac{l_d}{h_m}\right) \geq 1$	$Q_p = 1.102 - 0.05054\cdot\left(\frac{l_d}{h_m}\right) + 0.3054\cdot\left(\frac{h_m}{l_d}\right) - 1.65\cdot\mu + 0.005359\cdot\left(\frac{1}{\mu}\right) + 1.556\cdot\left(\frac{l_d}{h_m}\right)\cdot\mu$	0.96	0.06

Table C.2
Cold rolling model parameters.

ρ	7.6e-09 [t/mm^3]
c_p	645,750,000 [N*mm/t*K]
λ	28 [N/s*K]
Lever arm parameters C_1, C_2, C_3, C_4	0.62, −95, 720, 0.0008
Flow curve parameters (acc. to Hensel and Spittel) $A, A_1, A_2, A_3, A_4, A_5$	516.67, 0.0, 0.0, 0.0, 0.1141, 0.0

Appendix D. Uniaxial tensile testing of the cold strips

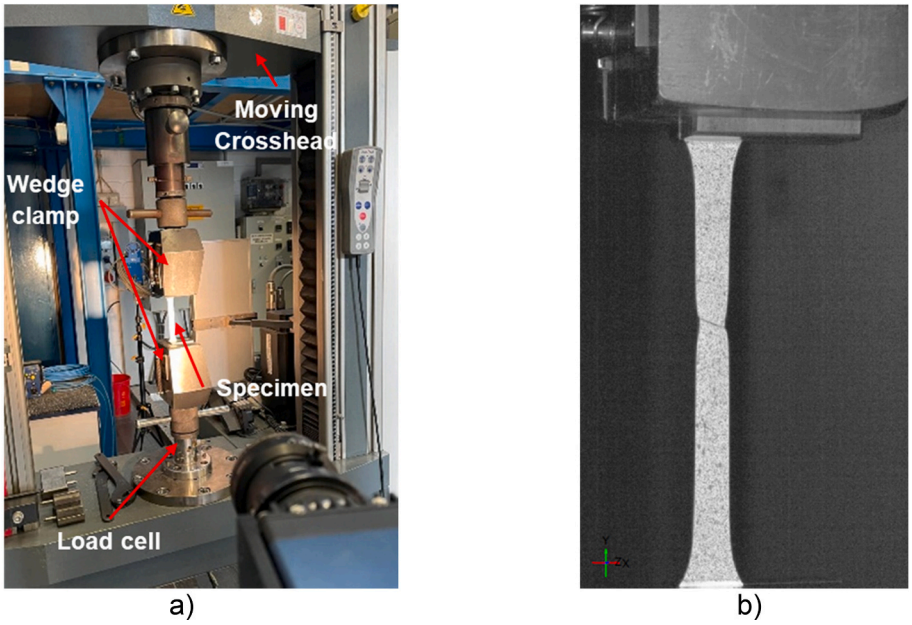

Fig. D.1. Experimental setup to conduct tensile tests a) Zwick 100 tensile testing machine together with Aramis optical measurement system to obtain the local strain distribution and b) tensile specimen during tensile testing. The use of measurement technique is shown in detail in [22].

Table D.2
Results of the characterization of the procured DC04 cold strips from three different suppliers using uniaxial tensile tests.

	Steel supplier A	Steel supplier B	Steel supplier C
Yield strength [MPa]	178	193	169
Tensile strength [MPa]	294	286	284
Poisson's ratio	0.31	0.33	0.29
Normal Anisotropy (r-value)	1.81	1.78	1.97
Hardening exponent (n)	0.23	0.19	0.21
Fracture strain [%]	26.85	24.83	24.44

Appendix E. Convergence and sensitivity analysis of the FE deep drawing model

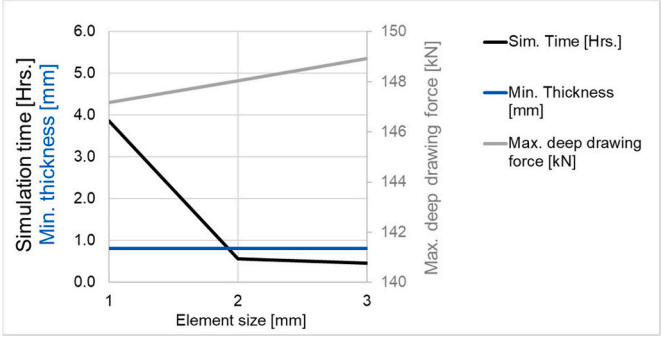

Fig. E.1. Convergence analysis to determine element size that is varied from 1.0 mm to 3 mm for square blank edge length of 300 mm and set blank holder force of 150 kN. Element size of 2 mm is selected because the simulation time is reduced by 3.3 h. and the difference in max. deep drawing force is 0.54 % w.r.t. mm element size of 1 mm.

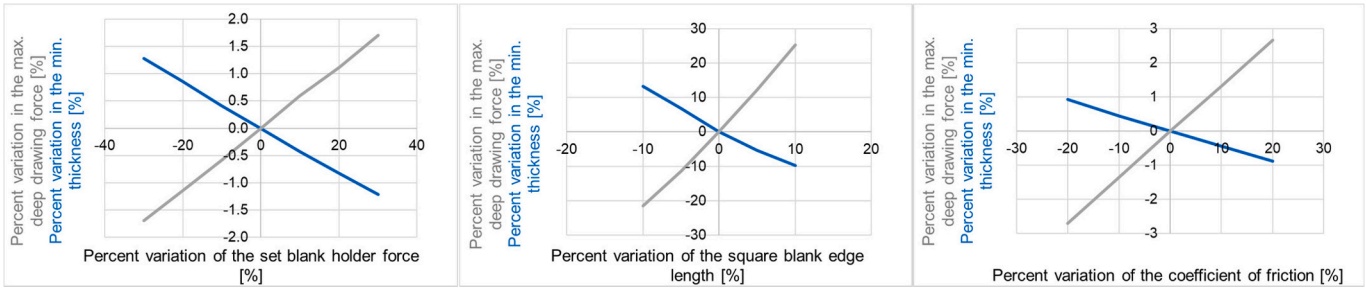

Fig. E.2. Sensitivity analysis to determine the influence of variation of the set blank holder force, square blank edge length and coefficient of friction on max. deep drawing force and min. thickness.

References

[1] Bakhshandeh P, Mohammadi Y, Altintas Y, Bleicher F. Digital twin assisted intelligent machining process monitoring and control. CIRP J. Manuf. Sci. Technol. 2024;49(2):180–90.

[2] Hafenecker J, Bartels D, Kuball C-M, Kreß M, Rothfelder R, Schmidt M, et al. Hybrid process chains combining metal additive manufacturing and forming – a review. CIRP J. Manuf. Sci. Technol. 2023;46(1):98–115.

[3] Powell D, Magnanini MC, Colledani M, Myklebust O. Advancing zero defect manufacturing: a state-of-the-art perspective and future research directions. Comput. Ind. 2022;136(10):103596.

[4] Beckers A, Stauder L, Grünebaum T, Barth S, Bergs T. Design of economically-optimized manufacturing process sequences using cross-process models. CIRP J. Manuf. Sci. Technol. 2021;33(6):15–29.

[5] Montgomery Douglas. Introduction to statistical quality control. 8th ed. John Wiley & Sons; 2020. 768 pp.

[6] Linnartz M, Leckel A. Data Sharing im Supply-Chain-Management: Ein Assistenzsystem für die Bewertung und Gestaltung der Offenheit und des Vertrauensniveaus zwischen Supply-Chain-Partnern. Zeitschrift für wirtschaftlichen Fabrikbetrieb 2020:563–6.

[7] Magnanini MC, Colledani M, Caputo D. Reference architecture for the industrial implementation of zero-defect manufacturing strategies. Procedia CIRP 2020;93 (2):646–51.

[8] Magnanini MC, Eger F, Reiff C, Colledani M, Verl A. A control model for downstream compensation strategy in multi-stage manufacturing systems of complex parts. IFAC-PapersOnLine 2019;52(13):1473–8.

[9] Beckers A, Hommen T, Becker M, Kornely MJK, Reuter E, Grünert G, et al. Digitalized manufacturing process sequences – foundations and analysis of the economic and ecological potential. CIRP J. Manuf. Sci. Technol. 2022;39(9): 387–400.

[10] IW Consult GmbH, 2017. Potentiale des digitalen Wertschöpfungsnetzes Stahl - Die Rolle der Stahlindustrie als Enabler der Digitalisierung der deutschen Wirtschaft.

[11] Fjodorovs N, Janßen J, Schröer T, Stich V, Thakare N, Lohmar J, et al. Überbetrieblicher Datenaustausch als Voraussetzung für adaptive Produktion. 36. Aachener Stahlkolloquium Umformtechnik; 2022. p. 293–302.

[12] Wisselink, H. & Niazi, Muhammad & Huetink, J., 2011. Validation of advanced material models using the crossdie test. Towards sustainable sheet forming processes, 1–10.

[13] Seuren S, Bambach M, Hirt G, Willkomm J, Bischof C, Bücker M. Analyse von Sensitivitäten bei der Modellierung des Grobblechwalzens. 2013.

[14] Seuren S, Philipp M, Bambach M, Hirt G. Determination of a geometric factor for the calculation of roll force in plate rolling by means of finite element simulations. 2009.

[15] Sellars CM, Whiteman JA. Recrystallization and grain growth in hot rolling. Metal Sci. J. 1979;13(3–4):187–94.

[16] Pavlina EJ, van Tyne CJ. Correlation of yield strength and tensile strength with hardness for steels. J. Mater. Eng. Perform. 2008;17(6):888–93.

[17] Sonmez, F.O., Demir, A., 2007. Analytical relations between hardness and strain for cold formed parts. JMPT 186 (1–3), 163–173.

[18] Douglas Montgomery, 2013. Design and analysis of experiments, Eighth edition ed. John Wiley & Sons Inc, Hoboken, NJ, 758 pp.

[19] Javorsky J, Franchetti M, Zhang H. Determining the optimal parameters of bonding polyvinylchloride to stainless steel in automotive applications with the use of full factorial design of experiment. CIRP J. Manuf. Sci. Technol. 2014;7(2):151–8.

[20] Seidenfeld T. R. A. Fisher on the design of experiments and statistical estimation. In: Cohen RS, Sarkar S, editors. The founders of evolutionary genetics. vol. 142. Dordrecht: Springer Netherlands; 1992. p. 23–36.

[21] Yarar E, Karabay S. Investigation of the effects of ultrasonic assisted drilling on tool wear and optimization of drilling parameters. CIRP J. Manuf. Sci. Technol. 2020;31 (1–3):265–80.

[22] Yashar Sarafraz, Malte Brink, Nikolas Baak, Alexander Koch, Frank Walther. Influence of pre-deformation on fatigue life of high strength steels by means of micromagnetic Barkhausen noise. https://doi.org/10.1515/mt-2022-0425.